SEMARAK ILMU PUBLISHING

Journal of Advanced Research in Applied Mechanics

Journal homepage:
https://semarakilmu.com.my/journals/index.php/appl_mech/index
ISSN: 2289-7895

Orientation of Linear Liquid Alkane on Solid Surface of Face Centered Cubic Lattice of (100), (110) and (111)

Ranjini Devi Rama[1], Abdul Rafeq Saleman[1,*], Muhamad Shukri Zakaria[1], Mohd Afzanizam Mohd Rosli[1], Bukhari Manshoor[2]

[1] Department of Mechanical Engineering, Faculty of Mechanical Engineering, Universiti Teknikal Malaysia Melaka, 75450 Ayer Keroh, Melaka, Malaysia
[2] Department of Mechanical Engineering, Faculty of Engineering and Manufacturing, Universiti Tun Hussein Onn Malaysia, 86400 Parit Raja, Batu Pahat, Johor, Malaysia

ARTICLE INFO

Article history:
Received 6 July 2024
Received in revised form 9 August 2024
Accepted 17 August 2024
Available online 30 August 2024

Keywords:
Solid-liquid interface; linear alkane; structural quantities

ABSTRACT

Solid-liquid (S-L) interfaces are found in numerous engineering applications, such as lubrication and coating systems as well as thermal interface materials. Understanding the interactions between (S-L) is crucial for optimizing various engineering applications. The main objective of this study is to provide insight regarding liquid adsorption on solid surfaces using non-equilibrium molecular dynamics simulations. To achieve this goal, a liquid confined between solid surfaces will be modeled to match the real state of contact interfaces using a constant temperature as a baseline. The results highlight a significant relationship between the peak height values of the liquid adsorption layer, density profile, and radius of gyration. Specifically, the peak height density at the S-L interfaces for the crystal plane (110) is 784.756 kg/m^3, followed by (100) at 801.786 kg/m^3, and finally the highest is for the crystal plane (111), at 966.940 kg/m^3. Whereas the radius of gyration at the S-L interfaces for crystal planes (100) and (111) is approximately 7.45×10^{-21} m^2, but for crystal plane (110) it is less and measures approximately 7.06×10^{-21} m^2. Conclusion, the adsorption layer of solid density near solid-liquid interfaces is significantly influenced by the peak height of the solid's density. Higher density results in a higher adsorption layer of liquid near solid-liquid interfaces. The number of solid density layers does not affect the height of adsorption layers for liquids.

1. Introduction

The border at the contact of a solid and a liquid is known as the solid-liquid (S-L) interface. S-L interfaces are commonly found in several engineering applications, such as thermal interface materials by jing *et al.,* [1, 2], lubrication and coating conducted by saleman *et al.,* [3], podulka *et al.,* [4], cooling of electronic equipment by shi *et al.,* [5], etc. Equilibrium and non-equilibrium properties of nanoscale materials on solid-liquid interfaces are key to the study of nanoscale materials. When

* *Corresponding author.*
E-mail address: rafeq@utem.edu.my

https://doi.org/10.37934/aram.124.1.152162

the interface thickness is measured in nanometers, comprehending macroscopic theory and physics becomes intricate and challenging due to the dominance of molecular exchanges between solid and liquid molecules by hilaire *et al.,* [6], lehmann *et al.,* [7], li *et al.,* [8]. Molecular dynamics (MD) simulations allow researchers to study the dynamic behavior of molecules in a controlled environment, providing insights into the properties and phenomena exhibited by nanoscale materials. By accurately shaping the interactions between atoms and molecules, MD simulations can help validate experimental findings and guide the design of new materials with tailored properties by z.xing *et al.,* [9], Anandakrishnan *et al.,* [10], rohl *et al.,* [11].

In previous research, MD simulations have demonstrated the dynamic behavior of liquids at the nanoscale level, allowing for a better understanding of how they interact with solid surfaces and enabling the development of more accurate models for predicting their behavior, such as liquid adhesion by nesbitt *et al.,* [12], wu *et al.,* [13], marta *et al.,* [14], liquid diffusion by elbourne *et al.,* [15], yang *et al.,* [16], and capillarity by li *et al.,* [17], Alharbi *et al.,* [18].

In past studies, the adsorption of liquid lubricant on solid surfaces by gao *et al.,* [19], kreivaitis *et al.,* [20] and the surface morphology of solid surfaces by hsu *et al.,* [21], olivares *et al.,* [22] were used to measure how well lubrication worked. However, a clear explanation of liquid adsorption and liquid orientation on solid surfaces at the molecular level has yet to be determined. Thus, this study investigates how the adsorption of linear alkane liquids interacts with solid surfaces that have different surface structures in a face-centered cubic (FCC) lattice with 100, 110 and 111 planes. To understand the adsorption processes, this research analyzes the structural variables of density distributions to evaluate the adsorption of liquid on solid surfaces.

2. Methodology

2.1 Model for the Simulation and Potential Functions

The simulation model is shown in Figure 1, presents a combination of two joined twin compact solid surfaces that are in contact with a linear alkane liquid of pentane (C_5H_{12}) between the solid walls. The solid walls are made of a face-centered cubic lattice (FCC) of gold (Au) with surfaces of (100), (110), and (111). This arrangement allows C_5H_{12} molecules to freely move within the space in between the solid walls without any interference. The 60Å spacing ensures that there is enough room for the C_5H_{12} molecules to move and interact with each other.

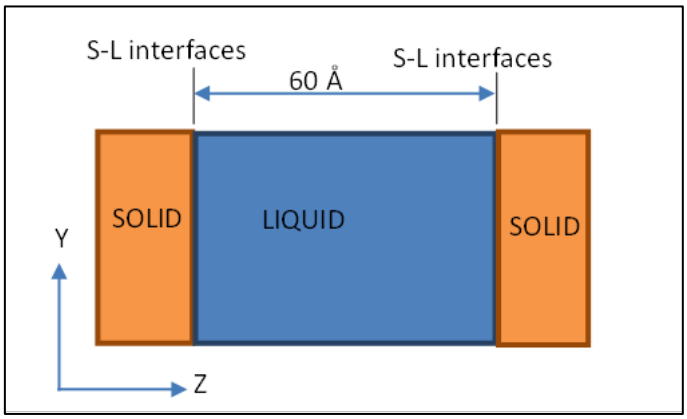

Fig. 1. Liquid in-between two parallel solid walls

In the simulation model, the united atom (UA) model of NERD potentials is used to represent the linear alkane liquid of C_5H_{12}. The same contact forces were applied in previous research by soltanahmadi *et al.,* [23, 24]. The related equation and detailed modeling of UA NERD potentials can

also be found in past studies by you *et al.,* [25], samant *et al.,* [26]. For the solid walls, Morse potentials were employed due to their ability to accurately describe the behavior of atoms at the interface. Morse potential can be modeled written as Eq. (1):

$$\Phi(\mathrm{r_{ij}}) = D\left[e^{-2\alpha(r_{ij}-r_0)} - 2e^{-\alpha(r_{ij}-r_0)}\right] \quad (1)$$

From the above equation, r_{ij} represents the distance of interaction between atoms *i* and *j*. The interaction of Au's free electron is not taken into consideration in this investigation. Although it was not considered, the influence is insignificant. The combined Lorentz-Bertholet principles are used to simulate the forces that interplay between solids and liquids. The same interactions and forces were employed in earlier research by xia *et al.,* [27], wu *et al.,* [28].

2.2 Details of the Simulation Process

The algorithm known as r-RESPA, short for Reversible Reference System Propagator Algorithm, is a widely accepted method for efficient and accurate time integration in molecular dynamics simulations. Using multiple time steps allows for a more realistic representation of both intermolecular and intramolecular interactions by yu *et al.,* [29]. This approach has been successfully applied in previous research by fernandes *et al.,* [30], selezneva *et al.,* [31] to investigate the dynamic behavior of solids and liquids at the atomic level.

In the beginning, the simulation system was slowly raised to the targeted temperature for 1–4 million-time steps. The temperature of the simulation system is controlled using velocity-scaling methods. Next, the simulation system was controlled and maintained at a uniform temperature of 0.7 T_c for the critical temperature (Tc) of the linear liquid alkane for 3–5 million-time steps. To verify the suitable molecule count placed in the simulation and to ensure that the linear alkane liquid behaves in a similar way as the actual liquid, the simulation system was managed at a uniform temperature of 0.7 T_c of the liquid. Data acquisitions were collected for the last step with a uniform temperature condition of 3-5 million interactions. After the data acquisition step, post-processing of the data is done. In post-processing, the calculation of the density and radius of gyration is evaluated according to the slab definition. A Flowchart of the simulation details is shown in Figure 2.

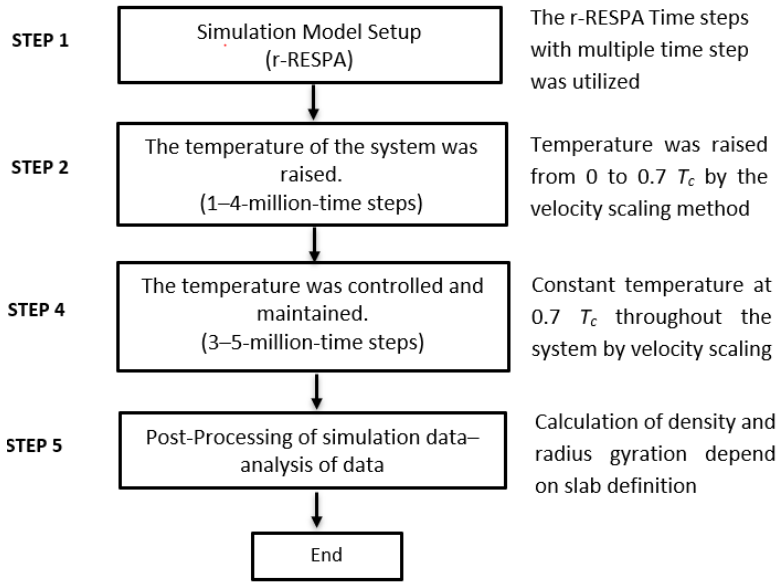

Fig. 2. Flowchart of representing the simulation process

3. Results and Discussion

3.1 Density Distributions

The density profile is the most important piece of information since it provides insight into the adsorption behavior of liquids at the center of systems and in the vicinity of solid surfaces. In these investigations, the simulation was divided into several layers parallel to the solid walls, which are referred to as slabs. The number of slabs is 5,900, and the thickness of each slab is approximately 0.01Å along the z-axis. The density distributions of the simulation systems are determined according to the quantity of CH_3 and CH_2 molecules found within each slab. Figure 3 presents the density distribution for C_5H_{12} liquid in contact with (100), (110), and (111) crystal planes.

According to Figure 3, for the crystal planes of (100) and (111), the solid structure layers were set to six; however, for the crystal plane of (110) they were set to ten layers. This setup was accomplished to ensure that all simulation systems, regardless of FCCs, have an approximately similar simulation system size. In the density profiles, the adsorption layer near the S-L interfaces for crystal plane of (100) has a peak height of 801.786 kg/m^3, while crystal plane of (110) shows a slightly lower peak at 784.756 kg/m^3. And the crystal plane of (111) exhibits the highest peak height, approximately 966.940 kg/m^3.However, the same density profile of solids has been observed for all three types of crystal planes, where the peak height of solid layers decreases as it moves towards the solid-liquid interfaces. This is due to the stronger fluctuation of solid molecules at solid-liquid interfaces. The same applies for the density profile of C_5H_{12}, regardless of the FCC in contact with the liquid. The density profile of liquid oscillates in the vicinity of the solid-liquid interface on both sides of the simulation system, and a flat line appears at the center of the system. The flat line is referred to as a bulk-like region. The same density profile for liquids and solids has been observed in previous studies by luz *et al.,* [32], pham *et al.,* [33].

As seen in Figure 3, the average peak height for the solid wall in (111) shows the highest value, followed by (100) and (110), which is expected since the number of molecules for each solid layer is different between FCCs, and (111) has the highest value and the highest number of molecules present in each solid layer. Regarding this setup, the adsorption layers for the liquid also experience the same trend, where the first peak of the liquid, which is located next to the solid-liquid interfaces, has the highest peak height for (111), followed by (100) and (110). Although the simulation systems exhibit approximately similar system sizes, the adsorption behavior of the liquid at the solid-liquid interfaces is different. Although the number of molecules for FCC (110) has the largest number of molecules present in each bulk solid, the adsorption layers of liquid adjacent to the solid layer show the lowest peak height. Thus, according to the results, the number of molecules in the liquid next to the liquid layer plays a significant role in determining the adsorption behavior of the liquid at the solid surfaces, which relates to the attraction and retraction forces between the solid and liquid.

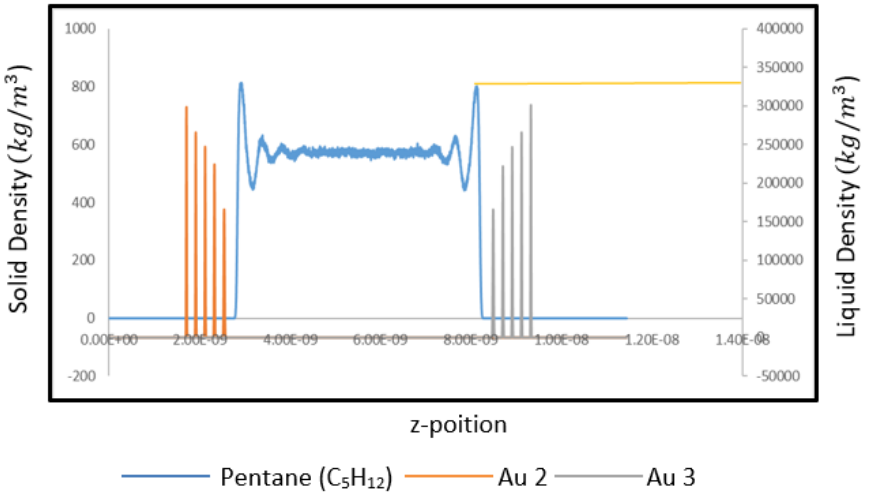

(a) FCC (100)

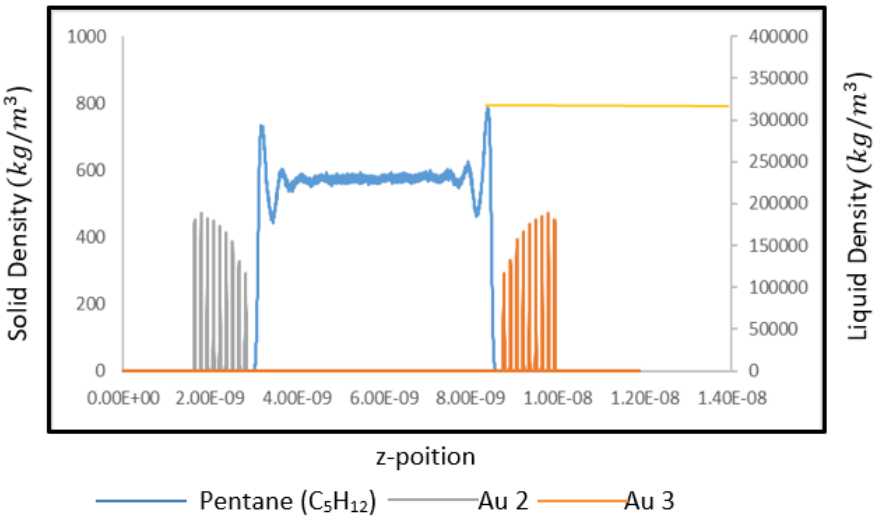

(b) FCC (110)

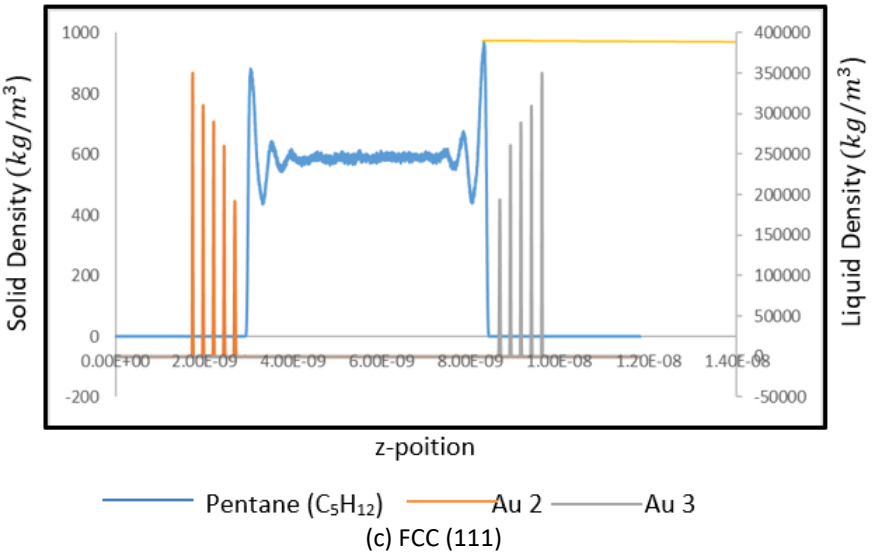

(c) FCC (111)

Fig. 3 Density profile of C_5H_{12} liquid in contact with the solid walls of (a) 100, (b) 110 and (c) 111

3.2 Radius of Gyration

The main function of the radius of gyration is to determine the shape and orientation of liquid in the x, y, and z directions. There are 5900 slabs, each with a thickness of roughly 0.01 Å along the z-axis. The density distributions of the simulation systems are determined by the number of CH_3 and CH2 molecules within each individual slab. Figure 4 presents the radius of gyration for C_5H_{12} pentane liquid facing the FCC lattice structure of the solid wall for (100), (110), and (111). The following Eq. (2) is to investigate the mean square radius gyration by joksimovic *et al.,* [34]. This equation can be expressed as (R^2) where *(N)* is the number of molecules, (r_{cp}) is the molecule from the center of mass in the position vector,$(\sum)$ is the overall number of molecules from the center of mass, (⟨ ⟩) is for combination, the average of a slab, and (r_i) is the united atom's position vector by bouchendouka *et al.,* [35].

$$R^2 = \frac{1}{N} \left\langle \sum_{i=1}^{N} (r_i - r_{cp})^2 \right\rangle \quad (2)$$

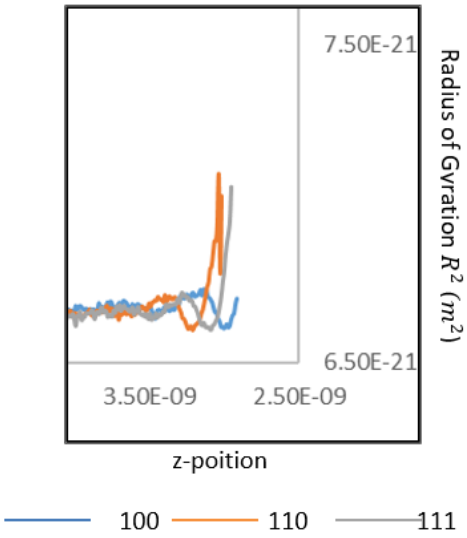

Fig 4. Radius of Gyration for C_5H_{12} on liquid and solid walls of (100), (110) and (111)

Based on Figure 4, the radius of gyration shows a high peak at the S-L interfaces for all types of FCCs. Whereas, in the center region, the value is approximately similar regardless of the FCCs. Since the radius of gyration profile is symmetrical on both the left and right sides of the simulation framework, only the right sides are shown in the figure. From the results, the crystal plane (110) is higher compared to the other two planes (110) and (111). The overall peak height of the radius of gyration near the S-L interfaces for each crystal plane is as follows, for (100) stands at 7.45×10^{-21} m^2, (110) at 7.47×10^{-21} m^2, and (111) at 7.06×10^{-21} m^2.

The radius of gyration further decomposes into the x-axis, y-axis, and z-axis for each crystal plane (100, 110, and 111) for liquid alkane C_5H_{12}, as shown in Figure 5 For each plane, the graph was organized as follows: (a), (b), and (c) are for the x-axis; (d), (e), and (f) for the y-axis; and (g), (h), and (i) for the z-axis, as shown on the solid surface.

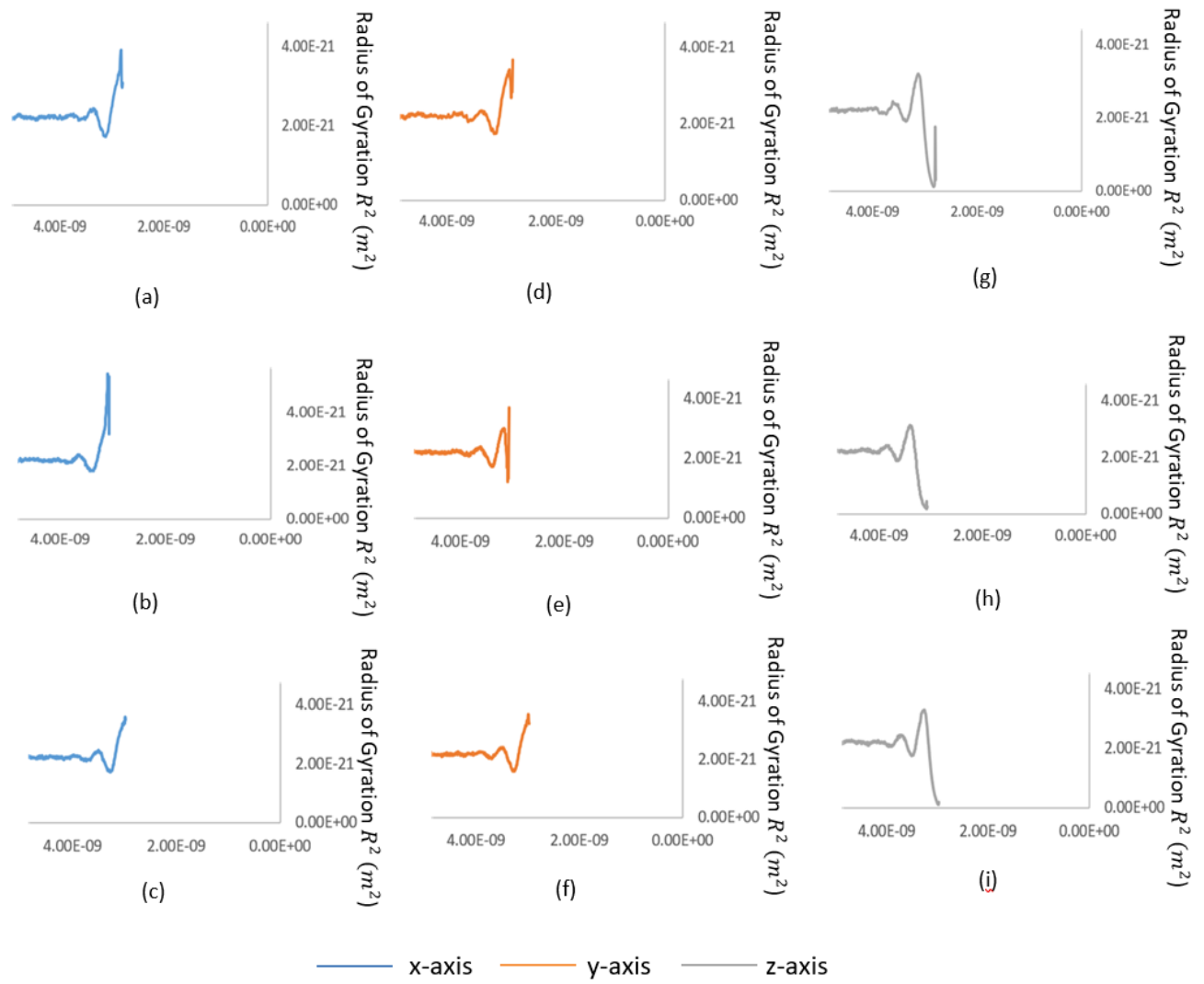

Fig 5. For each crystal plane (100, 110, and 111) for C_5H_{12} liquid alkanes, (a), (b) and (c) refer to the x-axis; (d), (e) and (f) for the y-axis; and (g), (h) and (i) for the z-axis

The results determined the behavior of liquid pentane (C_5H_{12}) molecules in contact with different crystal planes of a solid surface, focusing on the radius of gyration analysis along the x-axis by lobbert *et al.,* [36]. This analysis revealed the arrangement and interaction of liquid C_5H_{12} molecules across different crystal planes (100), (110), and (111). The key research finding is examining the radius of gyration analysis along the x-axis (a, b, and c), which indicates distinct behaviors of liquid C_5H_{12} molecules on the crystal planes. Although the peak heights of the radius of gyration for the (100) and (111) crystal planes are similar, the (110) crystal plane had a higher peak height. The higher peak on the (110) crystal plane introduces an interesting difference since it signifies a unique behavior of liquid C_5H_{12} molecules when positioned on this surface. The elevated peak suggests that liquid C5H12 molecules assume an extended arrangement along the x-axis on the (110) plane, differentiating their behavior from crystal planes (100) and (111). This difference in performance may be due to various factors. One possible explanation can be the unique atomic arrangement of the (110) plane, which can provide more available space and encourage liquid C_5H_{12} molecules to spread out and align along the x-axis. It is also believed that liquid C_5H_{12} molecules will experience stronger attractive forces or specific interactions with the (110) surface plane, leading to their extended arrangement along the x-axis.

The behavior of liquid pentane (C_5H_{12}) molecules on the y-axis at the solid surface of crystal planes (100), (110), and (111) is shown in (d), (e), and (f) of Figure 4. The main finding regarding the y-axis indicates that crystal planes of (100), (110), and (111) all share the same peak height in the radius of gyration analysis from simpson *et al.,* [37]. This uniformity in peak heights suggests the consistent behavior of liquid C_5H_{12} molecules across these different crystal planes along the y-axis. The liquid C_5H_{12} molecules revealed a similar vertical distribution and arrangement from the solid surface, irrespective of the specific atomic arrangement of the crystal planes.

Regarding the z-axis, the characteristics of liquid (C_5H_{12}) molecules within the bulk-like region for the above-mentioned crystal planes are presented in (g), (h), and (i) of Figure 4. The primary focus is to investigate the radius of gyration along the z-axis. The core study outcome revealed that the crystal planes of (100), (110), and (111) all share an identical peak height in the radius of gyration analysis. The uniform peak height suggests a consistent behavior of liquid C_5H_{12} molecules across different crystal planes along the z-axis within the centered region. This consistency indicates that the vertical distribution and arrangement of the liquid pentane particles on the solid surface remain unchanged, regardless of the specific atomic arrangement of the crystal planes by cheng *et al.,* [38]. This insight offers a deeper understanding of the interactions between these molecules and solid surfaces within the centered region. The fact that the peak heights remain constant on the crystal planes of (100), (110) and (111) indicates that the liquid C_5H_{12} molecules tend to arrange themselves in a similar manner along the vertical direction.

The same radius of gyration profile was observed in previous research papers from [39]. However, the researchers did not investigate the decomposed components of the radius of gyration. Based on our results for the y-axis and z-axis, the radius of gyration profile exhibited similar outcomes regardless of the crystal planes. While for the x-axis, the (110) crystal plane attained the highest value compared to the (100) and (111) crystal planes. This indicates that the alkane liquid was absorbed in the crystal structure of the (110) plane on the x-axis. Based on the surface structure of (110), elongated holes exist along the x-axis, which confirms that these holes were engaged by the liquid alkane C_5H_{12} molecules.

4. Conclusions

This study explored the behaviors of linear alkane liquids when interacting with three specific crystal planes: (100), (110), and (111). The main analysis provided an understanding of the density distribution and radius of gyration. These parameters were used to describe how liquid molecules are adsorbed near solid-liquid interfaces. The density profiles exhibited clear characteristics at these interfaces, indicating that the presence of molecules in the adsorption layers nearby the solid-liquid interfaces is affected by the quantity of molecules present in the layers where solid molecules interact with the liquid. Additionally, the radius of gyration has exhibited fluctuations in its results, which correlate with the lengths of the crystal planes of (100), (110) and (111). This research examined the way liquid pentane (C_5H_{12}) molecules interact with various crystal planes of a solid surface, with specific importance placed on examining how they behaved concerning the analysis of the radius of gyration along the x-axis, y-axis, and z-axis. The findings demonstrate that distinct behaviors characterize liquid pentane (C_5H_{12}) molecules on three types of crystal planes of a solid surface, with the (110) crystal plane displaying an extended arrangement along the x-axis, possibly due to its unique atomic arrangement and surface structure. Conversely, uniform behaviors are evident along the y-axis and z-axis, indicating consistent vertical distribution and arrangement across the (100), (110), and (111) crystal planes. As a conclusion, the adsorption layer of solid density near the solid-liquid interfaces is significantly influenced by the peak height of the solid's density, which

appears adjacent to the solid-liquid interfaces. The higher the solid's density appears near the solid-liquid interfaces, the higher the adsorption layer of liquid near the solid-liquid interfaces. The numbers of the solid's density layer do not affect the height of the adsorption layers of liquid near the solid-liquid interfaces. Additionally, the liquid is aligned in parallel with the solid surfaces, regardless of the crystal plane, and randomly oriented at the center of the liquid. These findings contribute to a deeper understanding of the adsorption phenomena and offer valuable implications for lubrication and coating systems in tribology, as well as the selection of various material combinations for thermal interface materials.

Acknowledgement
This research was funded by a grant from the Ministry of Higher Education of Malaysia and Universiti Teknikal Malaysia Melaka (FRGS/1/2022/TK05/UTEM/02/50).

References

[1] Jing, Lin, Rui Cheng, Raghav Garg, Wei Gong, Inkyu Lee, Aaron Schmit, Tzahi Cohen-Karni, Xu Zhang, and Sheng Shen."3D graphene-nanowire "sandwich" thermal interface with ultralow resistance and stiffness." *ACS nano* 17, no. 3 (2023): 2602-2610. https://doi.org/10.1021/acsnano.2c10525

[2] Jing, Lin, Rui Cheng, Muzaffer Tasoglu, Zexiao Wang, Qixian Wang, Hannah Zhai, Sheng Shen, Tzahi Cohen-Karni, Raghav Garg, and Inkyu Lee. "High Thermal Conductivity of Sandwich-Structured Flexible Thermal Interface Materials." *Small* 19, no. 11 (2023): 2207015. https://doi.org/10.1002/smll.202207015

[3] Saleman, Abdul Rafeq, Mohamad Shukri Zakaria, Ridhwan Jumaidin, and Mohd Nazmin Maslan. "Ultra-Thin Liquid Film with Shear and the Influences on Thermal Energy Transfer at Solid–Liquid Interfaces of Simple Liquid Methane in Contact With (110) Surface Structure of Face-Centred Cubic Lattice (FCC)." *Journal of Advanced Research in Fluid Mechanics and Thermal Sciences* 87, no. 3 (2021): 21-30. https://doi.org/10.37934/arfmts.87.3.2130

[4] Podulka, Przemysław, Wojciech Macek, Ricardo Branco, and Reza Masoudi Nejad. "Reduction in errors in roughness evaluation with an accurate definition of the SL surface." *Materials* 16, no. 5 (2023): 1865. https://doi.org/10.3390/ma16051865

[5] Shi, Limin, Tong Wang, Erliang Liu, and Ruyue Wang. "Lubrication mechanism of scCO2-MQL in the assisted machining of titanium alloys." *Machines* 11, no. 2 (2023): 291. https://doi.org/10.3390/machines11020291

[6] Hilaire, Lolita, Bertrand Siboulet, Sophie Charton, and Jean-François Dufrêche. "Liquid-liquid flow at nanoscale: Slip and hydrodynamic boundary conditions." *Langmuir* 39, no. 6 (2023): 2260-2273. https://doi.org/10.1021/acs.langmuir.2c02856

[7] Lehmann, Matthias. "Phase transitions in complex functional liquid crystals-the entropy effect." *Frontiers in Soft Matter* 3 (2023): 1089726. https://doi.org/10.3389/frsfm.2023.1089726

[8] Li, Hongyang, Ling Li, Jingang Zheng, Hao Huang, Han Zhang, Baigang An, Xin Geng, and Chengguo Sun. "Thermal Decomposition Assisted Construction of Nano-Li3N Sites Interface Layer Enabling Homogeneous Li Deposition." *ChemSusChem* 16, no. 13 (2023): e202202220.https://doi.org/10.1002/cssc.202202220

[9] Z. Xing, Li-Xin He, S. Liang, Lian-Bo Chang, Zhiyun Xiao, Wan-Li Xing, Haiying Shen, Jingjing Cao and Hong-Ji Liu. "Process Optimization of Dual-Liquid Casting and Interfacial Strength-Toughness of the Produced LAS/HCCI Bimetal." *Materials* 16 (2023). https://doi.org/10.3390/ma16052008

[10] Anandakrishnan, Abhijith, and Sarith P. Sathian. "A data driven approach to model thermal boundary resistance from molecular dynamics simulations." *Physical Chemistry Chemical Physics* 25, no. 4 (2023): 3258-3269. https://doi.org/10.1039/D2CP04551F

[11] Rohl, Susanne, Lena Hohl, Sebastian Stock, Manlin Zhan, Tobias Kopf, Regine von Klitzing, and Matthias Kraume. "Application of Population Balance Models in Particle-Stabilized Dispersions." *Nanomaterials* 13, no. 4 (2023): 698. https://doi.org/10.3390/nano13040698

[12] Nesbitt, David J., Alex M. Zolot, Joseph R. Roscioli, and Mikhail Ryazanov. "Nonequilibrium Scattering/Evaporation Dynamics at the Gas-Liquid Interface: Wetted Wheels, Self-Assembled Monolayers, and Liquid Microjets." *Accounts of Chemical Research* 56, no. 6 (2023): 700-711. https://doi.org/10.1021/acs.accounts.2c00823

[13] Wu, Jie, Zhiyuan Rui, Zhongyu Wang, and Yun Dong. "Temperature dependence of adhesion properties at liquid-aluminum/solid interfaces." *Journal of Physics: Condensed Matter* 35, no. 16 (2023): 165101. https://doi.org/10.1088/1361-648X/acbc03

[14] Marta Martín-García, J. Aguilera-Correa, M. Arenas, I. García-Diego, A. Conde, J. D. de Damborenea and J. Esteban. "Differences in In Vitro Bacterial Adherence between Ti6Al4V and CoCrMo Alloys." *Materials* 16 (2023). https://doi.org/10.3390/ma16041505

[15] Elbourne, Aaron, Madeleine Dupont, Rashad Kariuki, Nastaran Meftahi, Torben Daeneke, Tamar L. Greaves, Christopher F. McConville et al. "Mapping the Three-Dimensional Nanostructure of the Ionic Liquid-Solid Interface Using Atomic Force Microscopy and Molecular Dynamics Simulations." *Advanced Materials Interfaces* 10, no. 7 (2023): 2202110. https://doi.org/10.1002/admi.202202110

[16] Yang, Jing, Mostafa Youssef, and Bilge Yildiz. "Charged species redistribution at electrochemical interfaces: a model system of the zirconium oxide/water interface." Physical Chemistry Chemical Physics 25, no. 8 (2023): 6380-6391. https://doi.org/10.1039/d2cp05566j

[17] Li, L., B. Lu, W. X. Xu, Z. H. Gu, Y. S. Yang, and D. P. Tan. "Mechanism of multiphase coupling transport evolution of free sink vortex." *Acta Phys. Sin* 72, no. 3 (2023): 034702. https://doi.org/10.7498/aps.72.20221991

[18] Alharbi, Hattan A., Bassim H. Hameed, Khaled D. Alotaibi, Saud S. Al-Oud, and Abdullah S. Al-Modaihsh. "Conversion of a mixture of date palm wastes to mesoporous activated carbon for efficient dye adsorption." *Materials Research Express* 10, no. 1 (2023): 015602. https://doi.org/10.1088/2053-1591/acb2b6

[19] Gao, Can, Lei Jiang, and Zhichao Dong. "Effect of Wettability and Adhesion Property of Solid Margins on Water Drainage." *Biomimetics* 8, no. 1 (2023): 60. https://doi.org/10.3390/biomimetics8010060

[20] Kreivaitis, Raimondas, Milda Gumbytė, Artūras Kupčinskas, Jolanta Treinytė, and Eglė Sendžikienė. "Synthesis and Tribological Properties of Bis (2-hydroxyethyl) ammonium Erucate as a Potential Environmentally Friendly Lubricant and Lubricant Additive." *Applied Sciences* 13, no. 6 (2023): 3401. https://doi.org/10.3390/app13063401

[21] Hsu, Chao-Chun, Liang Peng, Feng-Chun Hsia, Bart Weber, Daniel Bonn, and Albert M. Brouwer. "Molecular probing of the stress activation volume in vapor phase lubricated friction." *ACS Applied Materials & Interfaces* 15, no. 9 (2023): 12603-12608. https://doi.org/10.1021/acsami.3c00789

[22] Olivares, Tulio, Zach Turi, and Brandon Hayes. "Innovative Solid Lubricant Solution to Reduce Friction in Challenging ERD wells." In *SPE Middle East Oil and Gas Show and Conference*, p. D031S100R001. SPE, 2023. https://doi.org/10.2118/213557-ms

[23] S. Soltanahmadi, M. Bryant and A. Sarkar. "Insights into the Multiscale Lubrication Mechanism of Edible Phase Change Materials." *ACS Applied Materials & Interfaces* 15 (2023): 3699-3712. https://doi.org/10.1021/acsami.2c13017

[24] Soltan Ahmadi, Siavash, Michael Bryant, and Anwesha Sarkar. "Insights into the multiscale lubrication mechanism of edible phase change materials." *ACS Applied Materials & Interfaces* 15, no. 3 (2023): 3699-3712. https://doi.org/10.1021/acs.jctc.2c01024

[25] You, Qianyu, Shun Gu, and Xiaofan Gou. "The highly accurate interatomic potential of CsPbBr3 perovskite with temperature dependence on the structure and thermal properties." *Materials* 16, no. 5 (2023): 2043. https://doi.org/10.3390/ma16052043

[26] Samant, R., S. U. Lotliker, and A. M. Desai. "Comments on the paper 'Comparison study of bound states for diatomic molecules using Kratzer, Morse, and modified Morse potentials." *Physica Scripta* 98, no. 2 (2023): 027002. https://doi.org/10.1088/1402-4896/acaa66

[27] Xia, Sheng-Yuan, Liang-Yan Guo, Lu-Qi Tao, Yunfeng Long, Zhengyong Huang, Jianfa Wu, and Jian Li. "Self-powered paper-based pressure sensor driven by triboelectric nanogenerator for detecting dynamic and static forces." *IEEE Transactions on Electron Devices* 70, no. 2 (2022): 732-738. https://doi.org/10.1109/TED.2022.3225129 .

[28] Wu, H., Y. Dai, and M. D. Ding. "Highly energetic electrons accelerated in strong solar flares as a preferred driver of sunquakes." *The Astrophysical Journal Letters* 943, no. 1 (2023): L6. https://doi.org/10.3847/2041-8213/acb0d1 .

[29] Yu, Xiaoqing, Kuo-Yang Chiang, Chun-Chieh Yu, Mischa Bonn, and Yuki Nagata. "On the Fresnel factor correction of sum-frequency generation spectra of interfacial water." *The Journal of Chemical Physics* 158, no. 4 (2023). https://doi.org/10.1063/5.0133428 .

[30] Fernandes, Joana Filipa Teixeira, Diamantino Freitas, Arnaldo Candido Junior, and João Paulo Teixeira. "Determination of harmonic parameters in pathological voices—efficient algorithm." *Applied Sciences* 13, no. 4 (2023): 2333. https://doi.org/10.3390/app13042333

[31] Selezneva, Elena, Irina Makarova, Radmir Gainutdinov, Alla Tolstikhina, Inna Malyshkina, Nikolai Somov, and Evgeniy Chuprunov. "Conductivity, its anisotropy and changes as a manifestation of the features of the atomic and real structures of superprotonic [K1–x (NH4) x] 3H (SO4) 2 crystals." *Acta Crystallographica Section B: Structural Science, Crystal Engineering and Materials* 79, no. 1 (2023): 46-54. https://doi.org/10.1107/s2052520622011751

[32] Luz, Arthur Mussi, Gabriel Barbosa, Carla Manske, and Frederico Wanderley Tavares. "Tween-80 on water/oil interface: structure and interfacial tension by molecular dynamics simulations." *Langmuir* 39, no. 9 (2023): 3255-3265. https://doi.org/10.1021/acs.langmuir.2c03001

[33] Pham, Dinh Quoc Huy, Mateusz Chwastyk, and Marek Cieplak. "The coexistence region in the Van der Waals fluid and the liquid-liquid phase transitions." *Frontiers in Chemistry* 10 (2023): 1106599. https://doi.org/10.3389/fchem.2022.1106599

[34] Joksimovic, Marija Gajevic, J. Benedikt Schmidt, Ilia V. Roisman, Cameron Tropea, and Jeanette Hussong. "Impact of a suspension drop onto a hot substrate: diminution of splash and prevention of film boiling." *Soft Matter* 19, no. 7 (2023): 1440-1453. https://doi.org/10.1039/d2sm01038k

[35] Bouchendouka, Abdellah, Zine El Abiddine Fellah, Zakaria Larbi, Nicholas O. Ongwen, Erick Ogam, Mohamed Fellah, and Claude Depollier. "A Generalization of Poiseuille's Law for the Flow of a Self-Similar (Fractal) Fluid through a Tube Having a Fractal Rough Surface." *Fractal and Fractional* 7, no. 1 (2023): 61. https://doi.org/10.3390/fractalfract7010061

[36] Lobbert, Laura, Saumil Chheda, Jian Zheng, Navneet Khetrapal, Julian Schmid, Ruixue Zhao, Carlo A. Gaggioli et al. "Influence of 1-butene adsorption on the dimerization activity of single metal cations on UiO-66 nodes." *Journal of the American Chemical Society* 145, no. 2 (2023): 1407-1422. https://doi.org/10.1021/jacs.2c12192

[37] Simpson, Grant J., Víctor García-López, A. Daniel Boese, James M. Tour, and Leonhard Grill. "Directing and Understanding the Translation of a Single Molecule Dipole." *The Journal of Physical Chemistry Letters* 14, no. 10 (2023): 2487-2492. https://doi.org/10.1021/acs.jpclett.2c03472

[38] Cheng, Cuixia, Yadong Zhou, Holden M. Nelson, Tasneem Ahmadullah, Hailan Piao, Zhaoying Wang, Wenxiao Guo, Jun-Gang Wang, Guosong Lai, and Zihua Zhu. "Molecular identification of wines using in situ liquid SIMS and PCA analysis." *Frontiers in Chemistry* 11 (2023): 1124229. https://doi.org/10.3389/fchem.2023.1124229

[39] Ribeiro, Daniela, A. R. R. Silva, and M. R. O. Panao. "Criterion for bubble encapsulation on drop impact onto a liquid film." *Physics of Fluids* 35, no. 3 (2023). https://doi.org/10.1063/5.0138901